To appear in Journal of The Structural Design of Tall and Special Buildings (John Wiley)

High-Performance Control of Wind-Induced Vibration of High-Rise Building via Innovative High-Hardness Rubber Damper

T. Tani, S. Yoshitomi, M. Tsuji, I. Takewaki *

Dept. of Urban & Environmental Eng., Graduate School of Eng., Kyoto University, Kyotodaigaku-Katsura, Nishikyo, Kyoto 615-8540, Japan

SUMMARY

High-hardness visco-elastic rubber dampers are used to upgrade both the habitability environment and the structural safety in high-rise buildings subjected to wind disturbances. While most of usual visco-elastic dampers have limitation on temperature and frequency dependencies, etc., the proposed high-hardness visco-elastic rubber dampers possess many unprecedented properties. High hardness, large stiffness, small temperature and frequency dependencies are examples of such properties.

Mechanical modeling of the proposed high-hardness visco-elastic rubber dampers is introduced first and the wind-induced response of high-rise buildings with and without the proposed high-hardness visco-elastic rubber dampers is computed under dynamic horizontal loads derived from wind-tunnel tests. It is shown that the high-rise buildings with the proposed high-hardness visco-elastic rubber dampers exhibit extremely smaller wind-induced responses (both along-wind and cross-wind responses) than those without such dampers. In particular, a remarkable reduction of acceleration has been achieved owing to sufficient hysteresis even in the small strain range. It is concluded that the proposed high-hardness visco-elastic rubber dampers can upgrade the habitability environment of building structures dramatically.

Keywords: Wind-induced response, Passive response control, High-hardness rubber, Visco-elastic damper, High-rise building, Habitability condition

* Corresponding author. Tel.: +81-75-383-3294, Fax: +81-75-383-3297,
E-mail: takewaki@archi.kyoto-u.ac.jp

1. Introduction

Visco-elastic dampers are often used as effective passive energy dissipation devices for wind and earthquake loading (for example, Zhang et al. 1989; Lin et al. 1991; Zhang and Soong 1992; Tsai and Lee 1993; Bergman and Hanson 1993; Chang et al. 1993; Kasai et al. 1993; Housner et al. 1994; Tsai 1994; Samali and Kwok 1995; Soong and Dargush 1997; Housner et al. 1997; Kobori et al. 1998; Hanson and Soong 2001; Casciati 2002; Uetani et al. 2003; Li et al. 2004; Chan and Chui 2006; Johnson and Smyth 2006; Tsuji et al. 2006). While many kinds of visco-elasic dampers have been proposed, there still remain several issues to be resolved. For example, most of usual visco-elastic dampers have limitation on temperature and frequency dependencies, etc. To overcome some of these issues, a new high-hardness visco-elastic rubber damper (Tsuji et al. 2006) (SRI rubber damper produced by SRI Hybrid Corporation, Japan) is proposed in this paper. High hardness, large stiffness, small temperature and frequency dependencies are examples of advantageous features of the proposed high-hardness visco-elastic rubber dampers.

Mechanical modeling of the proposed high-hardness visco-elastic rubber dampers is introduced first. The proposed model consists of three elements; i.e. (1) elastic-plastic element, (2) elastic element due to dynamic effect, (3) viscous element. The model parameters are determined based on the comparison with experimental results. The wind-induced response of high-rise buildings with and without the proposed high-hardness visco-elastic rubber dampers is computed under dynamic horizontal loads derived from wind-tunnel tests. Sophisticated treatment may be necessary in order to develop a computer program taking into account complicated mechanical characteristics of the proposed high-hardness visco-elastic rubber dampers. Furthermore, to the best of the authors' knowledge, it has never been conducted to compute the wind-induced response of the building including such complicated visco-elastic constitutive properties under realistic wind disturbances with the verification by wind-tunnel tests.

It is shown that the high-rise buildings with the proposed high-hardness visco-elastic rubber dampers exhibit extremely smaller along-wind and cross-wind responses under realistic wind disturbances than those without such dampers. Especially the reduction of

acceleration is remarkable owing to the sufficient hysteretic property of the proposed high-hardness visco-elastic rubber dampers even in the small strain range. This performance can help structural designers upgrade dramatically the habitability environment in high-rise buildings.

The proposed high-hardness visco-elastic rubber dampers have another advantage to be effective for overall flexural deformation of high-rise building frames. This comes from the fact that the present rubber damper exhibits a yielding-type force-deformation property and keeps a good performance even for the model taking into account the effect of overall flexural deformation of the building frame. The other advantages are (1) to have a yielding-type force-deformation property and play a role as a relief mechanism in viscous oil dampers in order to avoid the extreme force-transmission into neighboring structural members, (2) to have a large initial stiffness comparable to hysteretic steel panel dampers.

2. Mechanical modeling of high-hardness visco-elastic rubber dampers

2.1 Stationary loop

The proposed high-hardness visco-elastic rubber dampers exhibit peculiar characteristics compared to ordinary visco-elastic dampers and a new mechanical model is constructed in this paper.

The proposed model consists of three elements as shown in Fig.1(a): (1) elastic-plastic element, (2) elastic element due to dynamic effect (approximately frequency-independent property in the frequency range of interest), (3) viscous element. The elastic-plastic element expresses the strain dependency. The stiffness in the frequency range about 0.2-2.0Hz exhibits a value different from the static stiffness and can be regarded to be approximately constant. The elastic element due to dynamic effect expresses this property. The viscous element represents the viscosity of the material. The relations of shear stress τ with shear strain γ (or shear strain velocity $\dot{\gamma}$) in these three elements can be modeled as follows (shear stress τ :N/mm^2).

(1) elastic-plastic element (element 1)

Skeleton curve: $\tau = 0.32\,\mathrm{sgn}(\gamma)|\gamma|^{0.38}$ (1)

Re-yielding curve: $\tau = 0.11\,\mathrm{sgn}(\gamma)|\gamma|^{0.38}$ (2)

Unloading slope: $k_u = \dfrac{0.32 - 0.11\varepsilon^{0.38}}{(1-\varepsilon)\gamma_{\max}{}^{0.62}}$, $\varepsilon = \dfrac{0.94\gamma_{\max}{}^{0.73}}{\gamma_{\max}{}^{0.73} + 0.01}$ (3a,b)

Second-branch line: $\tau = \dfrac{0.32 - 0.11\varepsilon^{0.38}}{(1-\varepsilon)\gamma_{\max}{}^{0.62}}\gamma \pm \left(0.32 - \dfrac{0.32 + 0.11\varepsilon^{0.38}}{1+\varepsilon}\right)\gamma_{\max}{}^{0.38}$ (3c)

The definition of the skeleton curve, re-yielding curve, unloading slope k_u and second-branch line can be found in Fig.1(b) and $\gamma_{\max}$ indicates the maximum shear strain. In the virgin loading from the origin, the stiffness is defined by connecting the origin and the stress-strain point at $\gamma = 0.005$ on the skeleton curve.

(2) elastic element due to dynamic effect (element 2)

$$\tau = \begin{cases} 0.10\gamma_{\max}{}^{-0.66}\gamma & (\gamma_{\max} \geq 0.005) \\ 3.30\gamma & (\gamma_{\max} < 0.005) \end{cases} \quad (4)$$

(3) viscous element (element 3)

$$\tau = 5.1\times10^{-2}\,\mathrm{sgn}(\dot{\gamma})|\dot{\gamma}|^{0.202} \quad (5)$$

The elastic-plastic element, elastic element due to dynamic effect and viscous element will be called element 1, element 2 and element 3, respectively.

2.2 Non-stationary loop

The proposed high-hardness visco-elastic rubber dampers exhibit special characteristics for non-stationary loading and a sophisticated mechanical model should be constructed. The essence of the proposed model is the employment of reaction modification factors, applied to stationary-loop properties, for gradually decreasing loops. It has been observed from the experiment that such modification factors are unnecessary for gradually increasing loops because the maximum strain $\gamma_{\max}$ is updated successively in the gradually increasing loops.

The reaction shear stress in a stationary loop can be expressed by

$$\tau = \tau_1 + \tau_2 + \tau_3 \tag{6}$$

where τ_i denotes the reaction shear stress of element *i* in the stationary loop corresponding to $\gamma_{\max}$. On the other hand, the reaction shear stress in a non-stationary loop may be described by

$$\tau = \beta_2(\beta_1\alpha_1\tau_1 + \alpha_2\tau_2 + \alpha_3\tau_3) \tag{7}$$

where α_i = reaction modification factor of element *i* in a non-stationary loop, β_1=reaction magnification factor for the virgin loop and β_2=material randomness factor. α_1 expresses the reaction modification factor of element 1 defined for gradually decreasing loops. α_2 and α_3 represent the reaction modification factors of element 2 and 3, respectively.

The property of the present rubber damper depends on the ratio α of the amplitude γ_{re} in the last loop to the experienced maximum amplitude $\gamma_{\max}$ (Fig.2).

$$\alpha = \frac{\gamma_{re}}{\gamma_{\max}} \tag{8}$$

where

$$\gamma_{re} = \left| \frac{\gamma'_{re2} + \gamma'_{re1}}{2} \right| \quad \text{for} \quad \gamma'_{re2}/\gamma'_{re1} \geq 0 \tag{9a}$$

$$\gamma_{re} = \left| \frac{\gamma'_{re2} - \gamma'_{re1}}{2} \right| \quad \text{for} \quad \gamma'_{re2}/\gamma'_{re1} < 0 \tag{9b}$$

The reaction modification factor of element *i* in a non-stationary loop can then be expressed as

$$\alpha_1 = 0.855\alpha + 0.145 \tag{10}$$

$$\alpha_2 = \alpha^{-0.8} \tag{11}$$

$$\alpha_3 = \alpha^{0.4} \tag{12}$$

3. Comparison with experimental results

The accuracy of the mechanical model proposed in the previous section is verified

through the comparison with experiments conducted at SRI Hybrid Corporation (see Fig.3). The reaction magnification factor for the virgin loop is set as β_1=1.2 and the material randomness factor is specified as β_2=0.9 in this paper.

Fig.4 shows the experimental result for the reaction modification factor α_1 of element 1, indicated in Fig.5, for various shear strain amplitudes $\gamma_{\max}$. The lower bound is employed as the rule (Eq.(10)).

Fig.6 indicates the comparison of the model loop ((a) elastic-plastic element, (b) elastic-plastic element plus elastic element due to dynamic effect) with the experimental result. Fig.7 shows the experimental result for the reaction modification factor α_2 of element 2 for various shear strain amplitudes. An average curve has been employed as the rule.

Fig.8 presents the comparison of the model loop ((a) elastic-plastic element plus elastic element due to dynamic effect, (b) elastic-plastic element including elastic element due to dynamic effect plus viscous element) with the experimental result. Fig.9 shows the experimental result for the reaction modification factor α_3 of element 3 for various shear strain amplitudes $\gamma_{\max}$. As in the case of the coefficient α_2, an average curve has been employed as the rule.

In order to investigate the accuracy of the proposed rule for random loading, the comparison of the simulation with the corresponding experimental results has been made. The thickness of rubber dampers in this experiment is 5mm as shown in Fig.3. The comparison of the simulation with the experimental results for the strain smaller than 1.0 has been made before and good correspondence has been observed. In this paper the comparison for rather large strains is reported.

The ground motion of El Centro NS 1940 has been input to a standard 10-story shear building model and the interstory drift in the first story has been computed. For accuracy investigation, the interstory drift in the first story has been specified as a time history of forced displacement, i.e. a time history of forced shear strain, and the corresponding damper reaction has been evaluated. The interstory drift amplitude has been adjusted to 5, 10 and 15mm. The corresponding shear strains of rubber dampers are 1.0, 2.0, 3.0, respectively.

The case of 5mm is shown in Fig.10. Fig.11 shows the comparison of the simulated hysteresis by the proposed model with the experimental hysteresis for three amplitudes 5, 10 and 15mm. Fig.12 illustrates the comparison of the simulated time history of the damper reaction by the proposed model with the experimental time history. It can be observed that, while a small discrepancy can be found in the large amplitude, a fairly good correspondence can be seen. It may be concluded that the proposed material rule has a reasonable accuracy even for random loading.

4. Wind-induced response of high-rise buildings with and without the proposed high-hardness visco-elastic rubber dampers

A 40-story steel building frame, as shown in Fig.13, is treated here. The height is 160(m) and the plan is a square of 40(m) x 40(m). The floor mass is 1280×10^3(kg). The building without rubber dampers is designed by an optimization technique (Uetani et al. 2003) and the story stiffnesses of the building are shown in Fig.14. The fundamental natural period of the building without rubber dampers is 4.0(s) and the lowest-mode damping ratio of structural damping is 0.01.

The rubber dampers are provided as a wall-type damper system consisting of steel plates and rubber dampers as shown in Fig.15. The thickness of rubber dampers is 15(mm) and the area of the rubber dampers is 0.96(m^2). The building with 4 rubber-damper walls in every story is considered here.

To take into account the effect of overall flexural deformation as shown in Fig.15, the effective ratio of shear deformation in the total story deformation is introduced. These effective ratios have been evaluated by the frame analysis. As for the effect of local frame deformation around the rubber dampers, an additional effective ratio 0.9 is introduced throughout the height. The resulting total effective deformation ratios are shown in Fig.16. The quantities of the interstory drifts multiplied by these total effective deformation ratios coincide with the shear deformation of the rubber dampers.

In order to get the time-dependent horizontal nodal loads, the data by a wind tunnel test conducted at Takenaka Corporation in Japan have been used (Ohtake 2000). Three levels of

wind loads are set, (1) disturbance for Level 0 (1-year return period in Osaka, Japan: design wind velocity=23.5m/sec), (2) disturbance for Level 1 (50-year return period in Osaka, Japan: design wind velocity=47.0m/sec), (3) disturbance for Level 2 (500-year return period in Osaka, Japan: design wind velocity=58.8m/sec). Wind pressures at six representative heights (2-10 stories, 11-17 stories, 18-24 stories, 25-30 stories, 31-35 stories and 36-40 stories) were measured and those pressures were allocated to the corresponding stories. Fig.17 shows the along-wind time-history nodal loads for Level 0, Level 1 and Level 2. On the other hand, Fig.18 presents the cross-wind time-history nodal loads for Level 0, Level 1 and Level 2. In the wind tunnel test, the time starts at 0sec. At the first stage, a sudden loading effect appears. To eliminate this effect, the first 100sec has been removed.

The Newmark-β method (constant acceleration method) is used as the numerical integration scheme. The time interval of numerical integration is set as Δt =0.01 or 0.005(sec). The proposed high-hardness visco-elastic rubber dampers have very large initial stiffness and an instantaneous natural period of the total building model becomes much shorter than that of the bare frame. This phenomenon is conspicuous in the case of Level 0 loading. Therefore Δt = 0.005(sec) is used in analysis for Level 0 loading.

4.1 Along-wind disturbance

4.1.1 Level 0

Fig.19 shows the time histories of interstory drifts, horizontal displacements and accelerations at several representative floors (10, 20, 30, 40th stories) of the building without damper subjected to along-wind disturbances of Level 0 shown in Fig.17(a). On the other hand, Fig.20 presents the corresponding ones of the building with 4 proposed rubber walls in every story subjected to along-wind disturbances of Level 0. The total reaction force of the rubber dampers in the 10th story is also plotted with respect to the shear deformation (not the interstory drift) of the dampers. The maximum shear strain of the rubber damper is about 0.06. It should be pointed out that sufficient hysteresis can exist even in the small amplitude range in contrast to usual visco-elastic dampers. While the central points of displacement responses are in one side under along-wind disturbances, those of acceleration responses are

nearly at zero. This is due to the characteristics of along-wind disturbances. It can further be observed that the interstory drifts of the building with 4 rubber dampers in every story are smaller than those of the building without damper. This tendency is more remarkable in acceleration and the maximum acceleration has been reduced to one-fourth of the original. The habitability environment is closely related to acceleration and this performance of acceleration reduction can upgrade the habitability environment drastically.

The effect of overall flexural deformation of the frame on the performance of the rubber dampers will be investigated in Appendix.

4.1.2 Level 1

Figs.21 and 22 illustrate the corresponding time histories subjected to along-wind disturbances for Level 1 shown in Fig.17(b). The maximum shear strain of the rubber damper in the 10th story is about 0.31. Remarkable response reduction can also be observed in case of along-wind disturbances for Level 1. While the reduction of displacement responses is not so remarkable, the reduction of accelerations is remarkable (reduced to half of the original).

4.1.3 Level 2

Figs.23 and 24 show the corresponding time histories subjected to along-wind disturbances for Level 2 shown in Fig.17(c). The maximum shear strain of the rubber damper in the 10th story is about 0.54. Remarkable response reduction can also be observed in case of along-wind disturbances for Level 2. As in case of along-wind disturbances for Level 1, the reduction of accelerations is remarkable and reduced to half of the original.

4.2 Cross-wind disturbance

4.2.1 Level 0

Fig.25 presents the time histories of interstory drifts, horizontal displacements and accelerations at several representative floors (10, 20, 30, 40th stories) of the building without damper subjected to cross-wind disturbances of Level 0 shown in Fig.18(a). On the other

hand, Fig.26 shows the corresponding ones of the building with 4 rubber walls in every story subjected to cross-wind disturbances of Level 0. The total reaction force of the rubber dampers in the 10th story is also plotted with respect to the shear deformation of the dampers. The maximum shear strain of the rubber damper in the 10th story is about 0.03. In contrast to the case of along-wind disturbances, the central points of both displacement responses and acceleration responses are nearly at zero. This is due to the characteristics of cross-wind disturbances shown in Fig.18. It can further be observed that the interstory drifts of the building with 4 rubber dampers in every story are smaller than those of the building without damper (reduced to half of the original). This tendency is more remarkable in acceleration and the maximum acceleration has been reduced to one-fourth of the original. As in the case of along-wind disturbances, the habitability environment is related to acceleration and this performance of acceleration reduction can upgrade the habitability environment.

4.2.2 Level 1

Figs.27 and 28 show the corresponding time histories subjected to cross-wind disturbances for Level 1 shown in Fig.18(b). The maximum shear strain of the rubber damper in the 10th story is about 0.28. Remarkable response reduction can also be observed in case of cross-wind disturbances for Level 1. In contrast to the case of along-wind disturbances, both the displacement responses and accelerations are reduced to half of the original.

4.2.3 Level 2

Figs.29 and 30 illustrate the corresponding time histories subjected to cross-wind disturbances for Level 2 shown in Fig.18(c). The maximum shear strain of the rubber damper in the 10th story is about 0.56 and is larger than that for along-wind disturbances. Remarkable response reduction can also be observed in case of cross-wind disturbances for Level 2. In contrast to the case of along-wind disturbances, both the displacement responses and accelerations are reduced to half of the original.

5. Assessment of habitability environment

In order to assess the habilitability environment of the building with and without the proposed high-hardness visco-elastic rubber dampers, the maximum response acceleration is plotted in the assessment sheet (AIJ 2004) revised in Japan.

Fig.31 shows the plot of the maximum accelerations at the top floor in the building with and without the proposed high-hardness visco-elastic rubber dampers in the assessment sheet of the habitability environment. It can be observed that a remarkable upgrade of the habitability environment can be achieved by the appropriate installation of the proposed high-hardness visco-elastic rubber dampers. The level H-30 has been upgraded to the level H-10 for along-wind loading and the level H-50 has been upgraded to the level H-10 for cross-wind loading.

6. Conclusions

The conclusions may be summarized as follows:

(1) High-hardness visco-elastic rubber dampers can upgrade remarkably the habitability for wind disturbances in high-rise buildings.

(2) While most visco-elastic dampers have limitation on temperature and frequency dependencies, etc., the proposed high-hardness visco-elastic rubber dampers possess many unprecedented properties. High hardness, large stiffness, small temperature and frequency dependencies are the advantageous properties to be emphasized.

(3) A mechanical model of the proposed high-hardness visco-elastic rubber dampers has been constructed and its accuracy has been evaluated through the comparison with the corresponding experimental data.

(4) The wind-induced response of high-rise buildings with and without the proposed high-hardness visco-elastic rubber dampers has been computed under dynamic horizontal loads derived from wind-tunnel tests. It has been shown that the high-rise buildings with the proposed high-hardness visco-elastic rubber dampers exhibit extremely smaller wind-induced response (both along-wind and cross-wind responses) than those without such dampers. The performance can be understood in the assessment sheet of the

habitability environment.

(5) The proposed high-hardness visco-elastic rubber dampers have an advantage to be effective even for overall flexural deformation of high-rise building frames. This is because the present rubber damper exhibits a yielding-type force-deformation property and keeps a good performance even for the model taking into account the effect of overall flexural deformation of building frames.

(6) The other advantages of the proposed high-hardness visco-elastic rubber dampers are to have a yielding-type force-deformation property and play a role as a relief mechanism in viscous oil dampers in order to avoid the extreme force-transmission into neighboring structural members and to have a large initial stiffness comparable to hysteretic steel panel dampers.

ACKNOWLEDGEMENTS

The material experimental data of high-hardness visco-elastic rubber dampers were provided by SRI Hybrid Corporation, Japan and the data of the wind tunnel test were provided by Takenaka Corporation, Japan. Some useful comments have also been provided by Dr. Tatsuji Matsumoto of SRI Hybrid Corporation and Dr. Kazuo Ohtake of Takenaka Corporation. The authors are grateful to SRI Hybrid Corporation and Takenaka Corporation for these supports.

APPENDIX: Response of the model without effective shear-deformation coefficient (Level 0, along-wind direction)

In order to investigate the effect of overall flexural deformation of the frame on the performance of the rubber dampers, another model without the effect of overall flexural deformation of the frame is taken into account. In this model, the shear deformation of the rubber dampers coincides with the interstory drift. Fig.32 shows the interstory drifts, horizontal displacements, accelerations at 10th, 20th, 30th, 40th story levels and the reaction-deformation relation of the rubber dampers in the model with 4 rubber-damper walls subjected to the along-wind direction loading of Level 0 corresponding to Fig.20. It can be

observed that no remarkable difference is found. This is because the present rubber damper exhibits a yielding-type force-deformation property and keeps a good performance even for the model taking into account the effect of overall flexural deformation of the frame.

REFERENCES

Architectural Institute of Japan. 2004. *Guidelines for the evaluation of habitability to building vibration*.

Bergman DM, Hanson RD. 1993. Viscoelastic mechanical damping devices tested at real earthquake displacements, *Earthquake Spectra*, **9**(3): 389-418.

Casciati F (ed.) 2002. *Proc. of 3rd World Conf. on Structural Control*, Como (Italy), John Wiley & Sons Ltd.

Chan CM, Chui JKL. 2006. Wind-induced response and serviceability design optimization of tall steel buildings, *Engineering Structures*, **28**: 503-513.

Chang KC, Soong TT, Lai ML, Nielsen EJ. 1993. Viscoelastic dampers as energy dissipation devices for seismic applications, *Earthquake Spectra*, **9**(3): 371-388.

Hanson RD, Soong TT. 2001. *Seismic design with supplemental energy dissipation devices*, EERI monograph series MNO-8.

Housner GW, Masri SF, Chassiakos AG (eds.). 1994. *Proc. of 1st World Conf. on Structural Control*, Los Angeles (USA), IASC.

Housner GW et al. 1997. Special issue, Structural control: past, present, and future', *J. Engng. Mech. ASCE*, **123**(9): 897-971.

Johnson E, Smyth A (eds.) 2006. *Proc. of 4th World Conf. on Structural Control and Monitoring* (4WCSCM), San Diego (USA), 2006, IASC.

Kasai K, Munshi JA, Lai ML, Maison BF. 1993. Viscoelastic damper hysteretic model: theory, experiment and application, *Proc. ATC-17-1 on Seismic Isolation, Energy Dissipation, and Active Control*, Vol.2: 521-532.

Kobori T, Inoue Y, Seto K, Iemura H, Nichitani A (eds.). 1998. *Proc. of 2nd World Conf. on Structural Control*, Kyoto (Japan), John Wiley & Sons Ltd.

Li QS, Wu JR, Liang SG., Xiao YQ, Wong CK. 2004. Full-scale measurements and numerical evaluation of wind-induced vibration of a 63-story reinforced concrete tall building, *Engineering Structures*, **26**: 1779-1794.

Lin RC, Liang Z, Soong TT, Zhang RH. 1991. An experimental study of seismic behaviour of viscoelastically damped structures, *Engineering Structures*, **13**: 75-84.

Ohtake K. 2000. Peak wind pressure coefficients for cladding of a tall building, Part 1: Characteristics of peak wind pressure, *Annual meeting of Architectural Institute of Japan, Structural Branch I*, pp193-194.

Samali B, Kwok KCS. 1995. Use of viscoelastic dampers in reducing wind- and earthquake-induced motion of building structures, *Engineering Structures*, **17**(9): 639-654.

Soong TT, Dargush GF. 1997. *Passive energy dissipation systems in structural engineering*, John Wiley & Sons Ltd.

Tsai CS. 1994. Temperature effect of viscoelastic dampers during earthquakes, *J. Structural Engineering, ASCE*, **120**(2): 394-409.

Tsai CS, Lee HH. 1993. Application of viscoelastic dampers to highrise buildings, *J. Structural Engineering*, ASCE, **119**(4): 1222-1233.

Tsuji M, Tani T, Takewaki I, Matsumoto T. 2006. Habitability upgrade of buildings by visco-elastic damper using high-hardness rubber, *Proc. of the 12th Japan Earthquake Engineering Symposium*, pp970-973.

Uetani K, Tsuji M, Takewaki I. 2003. Application of Optimum Design Method to Practical Building Frames with Viscous Dampers and Hysteretic Dampers, *Engineering Structures*, **25**(5): 579-592.

Zhang RH, Soong TT. 1992. Seismic design of viscoelastic dampers for structural applications, *J. Structural Engineering*, ASCE, **118**(5): 1375-1392.

Zhang RH, Soong TT, Mahmoodi P. 1989. Seismic response of steel frame structures with added viscoelastic dampers, *Earthquake Engineering Structural Dynamics*, **18**: 389-396.

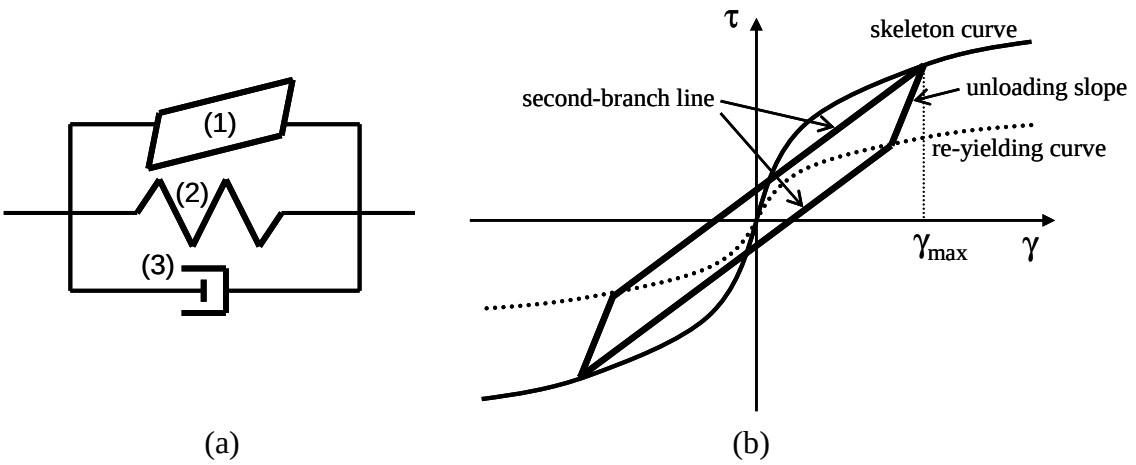

Fig.1 (a) Three elements in high-hardness visco-elastic rubber damper: (1) elastic-plastic element, (2) elastic element due to dynamic effect, (3) viscous element
(b) Definition of terminology in elastic-plastic element

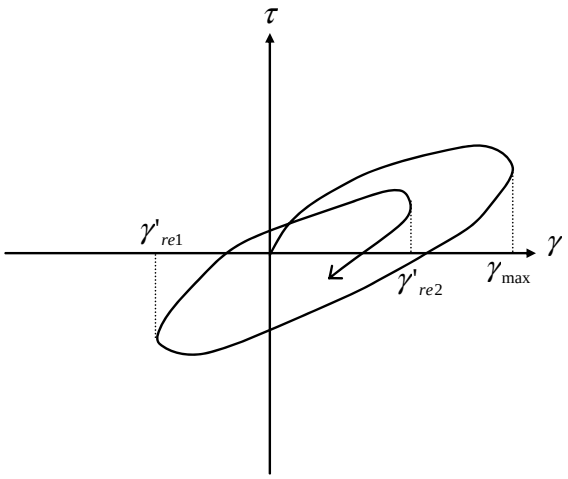

Fig.2 Arbitrary hysteresis loop and definition of strain amplitude ratio

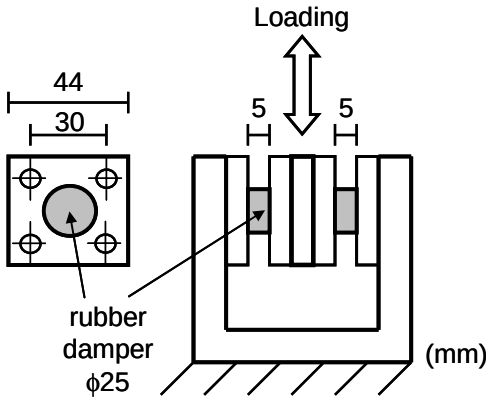

Fig.3 Schematic diagram of experimental set-up

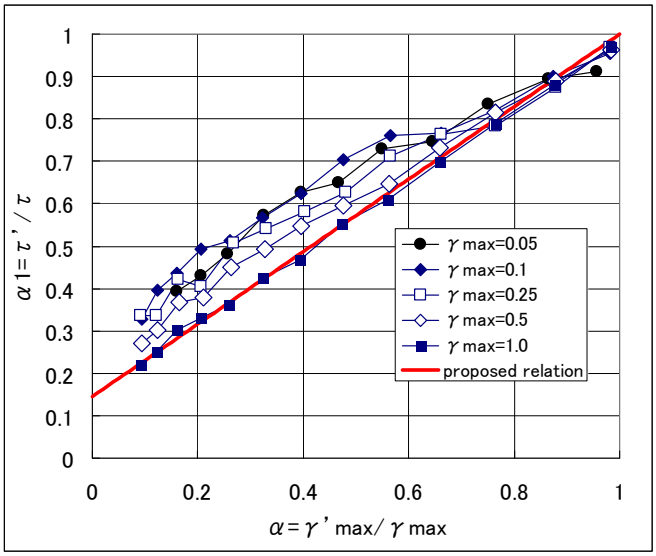

Fig.4 Experimental result for the reaction modification factor α_1 of element 1 and its modeling into an approximate formula

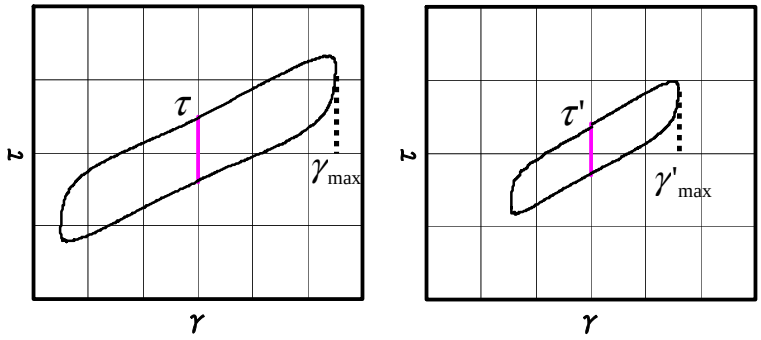

(a) (b)

Fig.5 Definition of reaction reduction τ'/τ with respect to strain amplitude ratio, (a) stationary loop of strain amplitude $\gamma_{\max}$, (b) subsequent arbitrary loop of strain amplitude $\gamma'_{\max}$

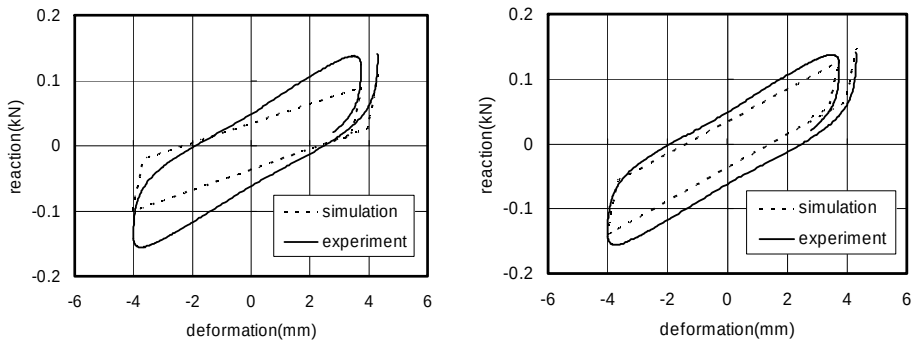

(a) (b)

Fig.6 Modeling accuracy in terms of one or two elements, (a) elastic-plastic element, (b) elastic-plastic element plus elastic element due to dynamic effect

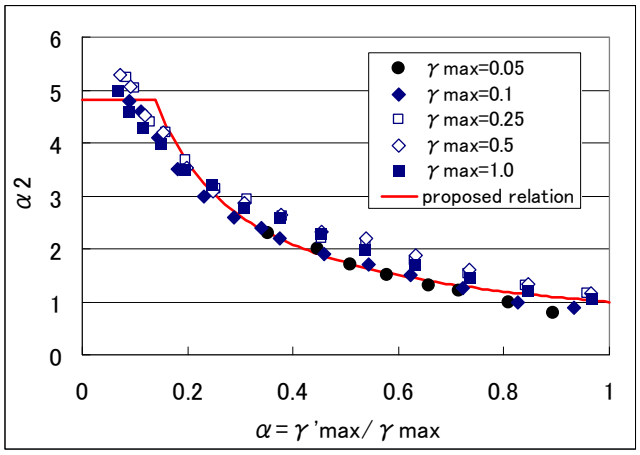

Fig.7 Experimental result for the reaction modification factor α_2 of element 2 and its modeling into an approximate formula

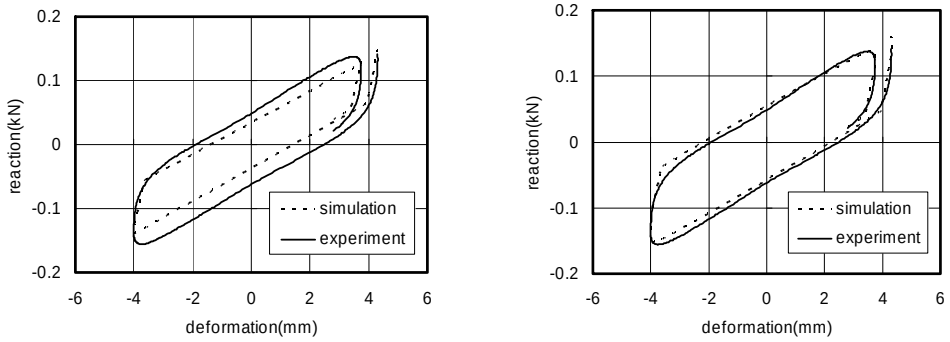

(a) (b)

Fig.8 Modeling accuracy in terms of two or three elements, (a) elastic-plastic element plus elastic element due to dynamic effect, (b) elastic-plastic element including elastic element due to dynamic effect plus viscous element

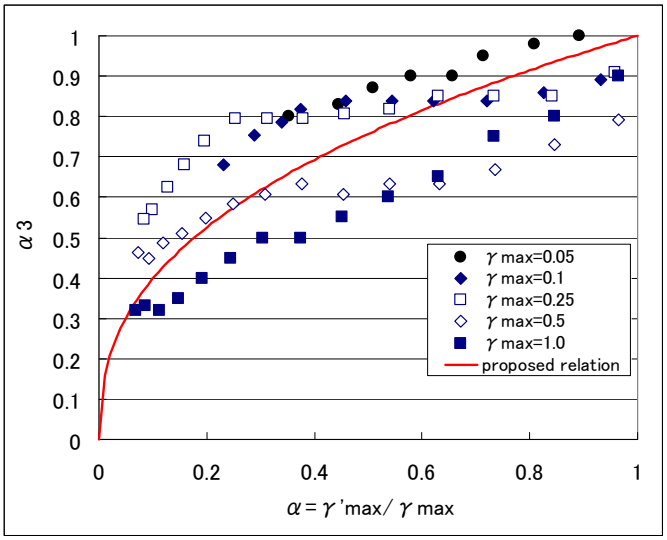

Fig.9 Experimental result for the reaction modification factor α_3 of element 3 and its modeling into an approximate formula

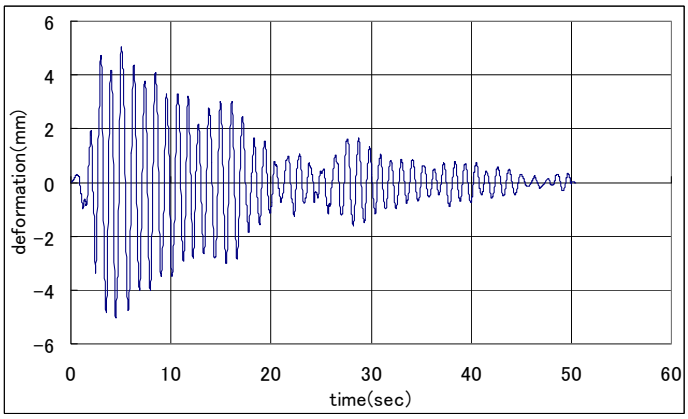

Fig.10 Interstory drift in the first story of a ten-story shear building model subjected to El Centro NS 1940 (amplitude is adjusted to 5mm)

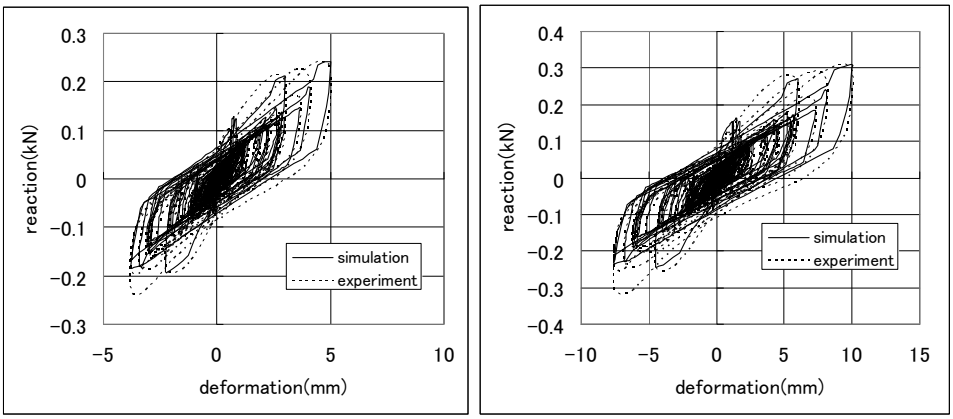

(a) (b)

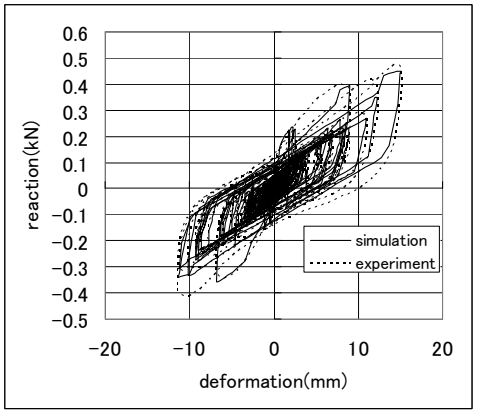

(c)

Fig.11 Comparison of the simulated hysteresis by the proposed model with the experimental hysteresis; (a) amplitude is adjusted to 5mm (strain=1.0), (b) amplitude is adjusted to 10mm, (c) amplitude is adjusted to 15mm

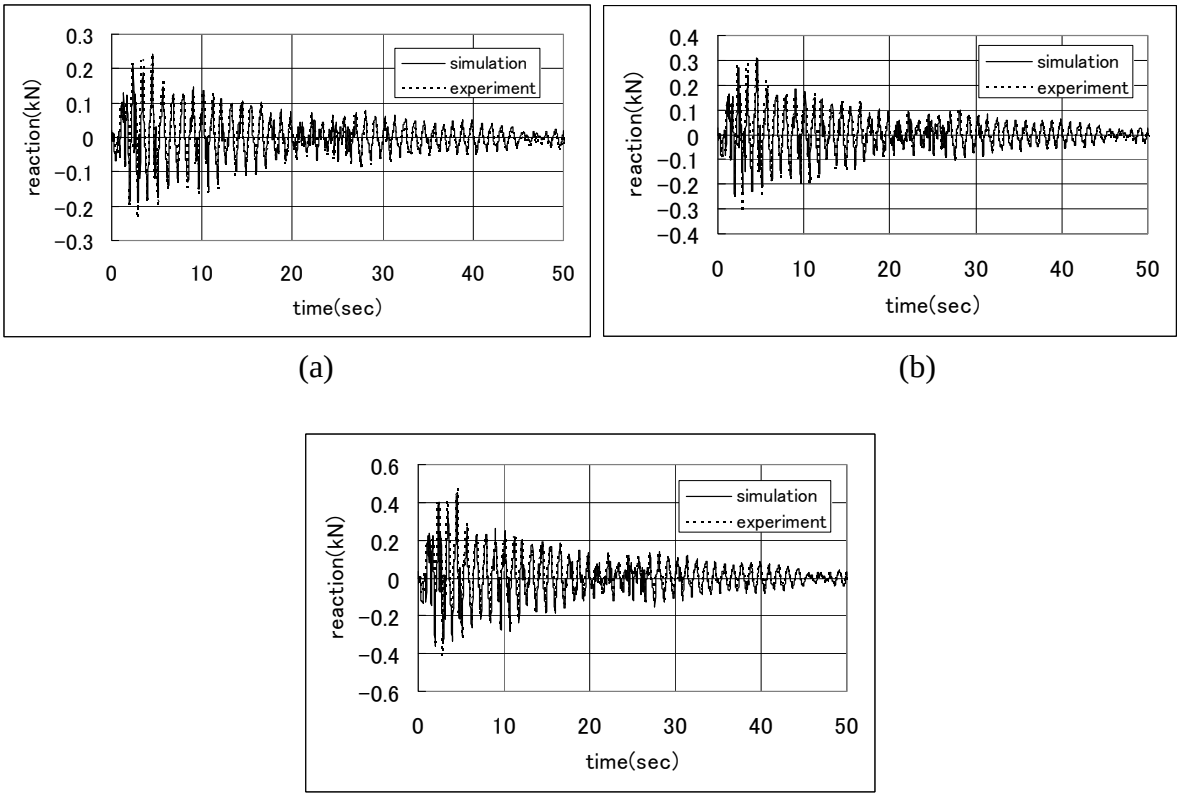

Fig.12 Comparison of the simulated time history of the damper reaction by the proposed model with the experimental time history; (a) amplitude is adjusted to 5mm (strain=1.0), (b) amplitude is adjusted to 10mm, (c) amplitude is adjusted to 15mm

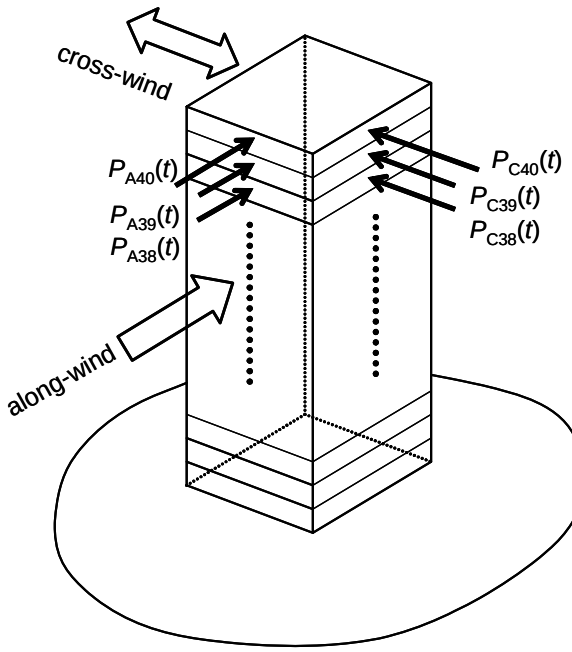

Fig.13 40-story building subjected to wind loading

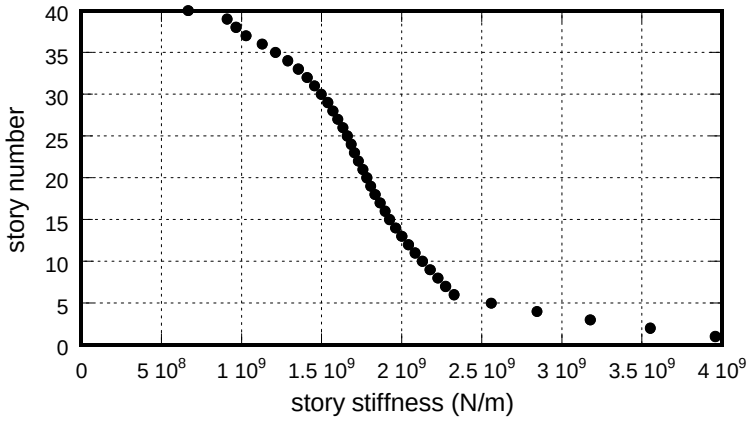

Fig.14 Story stiffness distribution

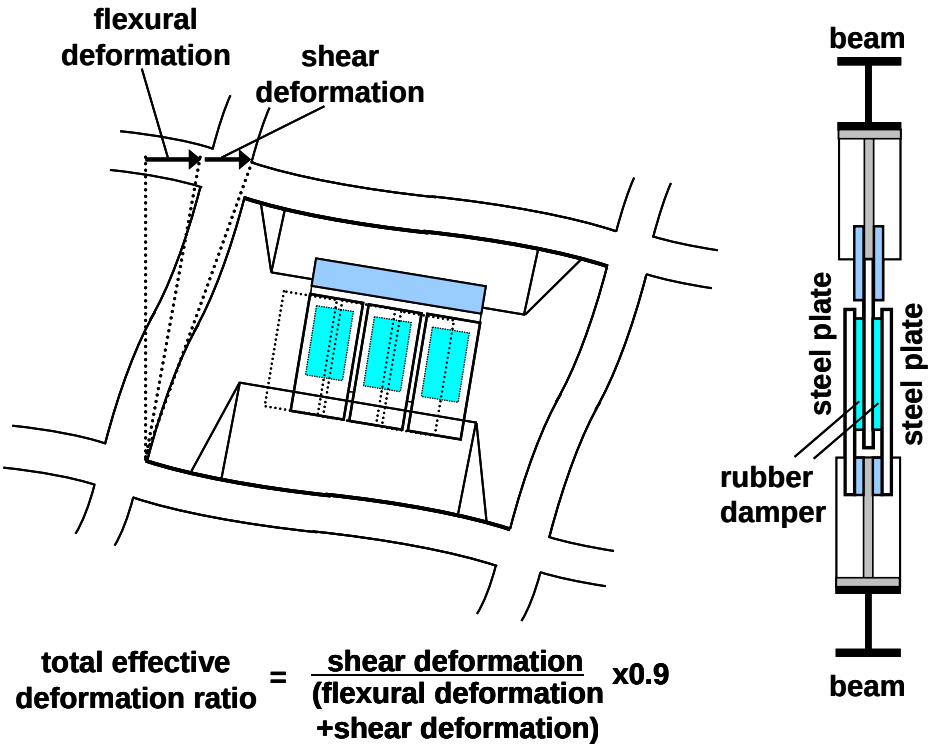

Fig.15 Overall flexural deformation, shear deformation and local supporting-member deformation

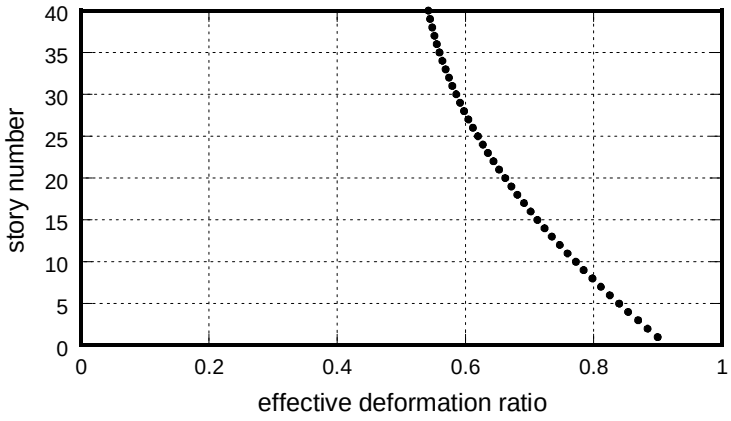

Fig.16 Effective deformation ratio distribution

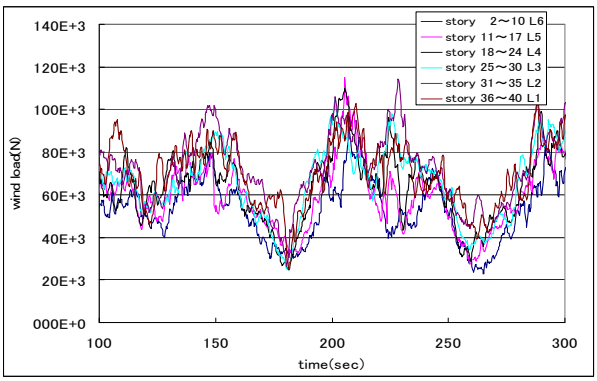

(a) Level 0 corresponding to 1-year return period

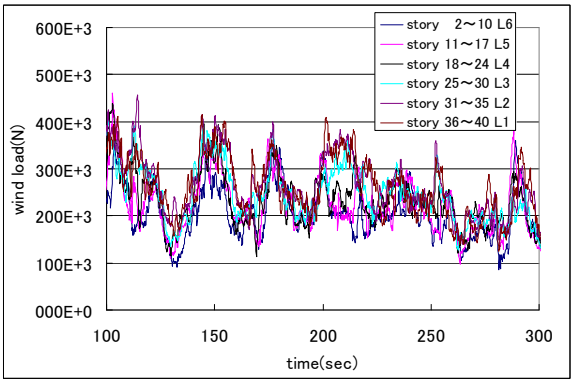

(b) Level 1 corresponding to 50-year return period

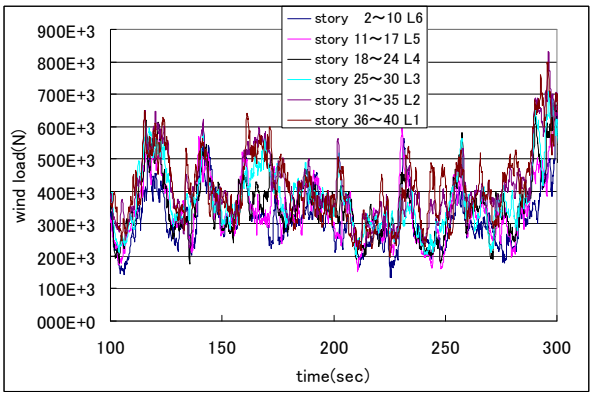

(c) Level 2 corresponding to 500-year return period

Fig.17 Time-dependent wind forces at various building height levels (along-wind direction)

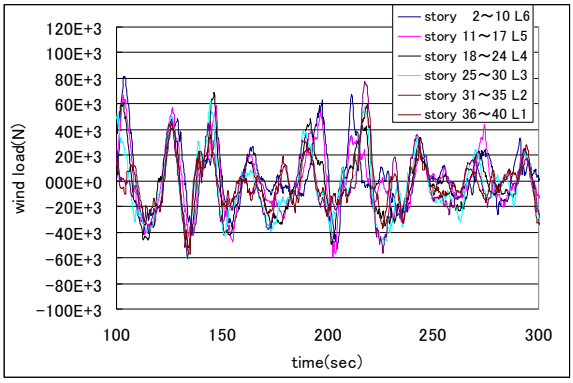

(a) Level 0 corresponding to 1-year return period

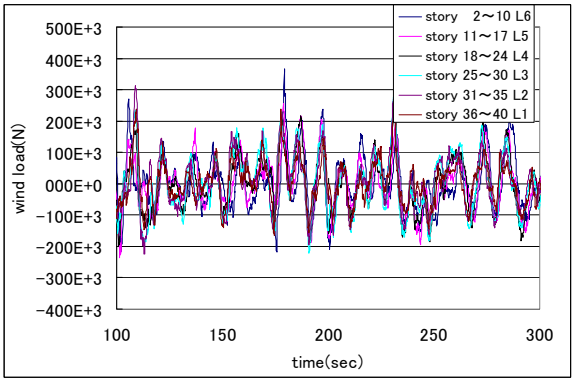

(b) Level 1 corresponding to 50-year return period

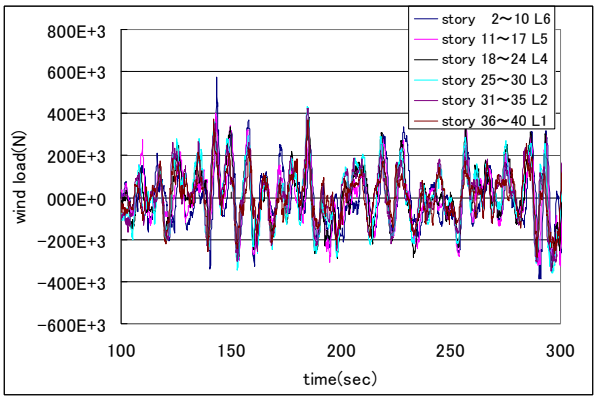

(c) Level 2 corresponding to 500-year return period

Fig.18 Time-dependent wind forces at various building height levels (cross-wind direction)

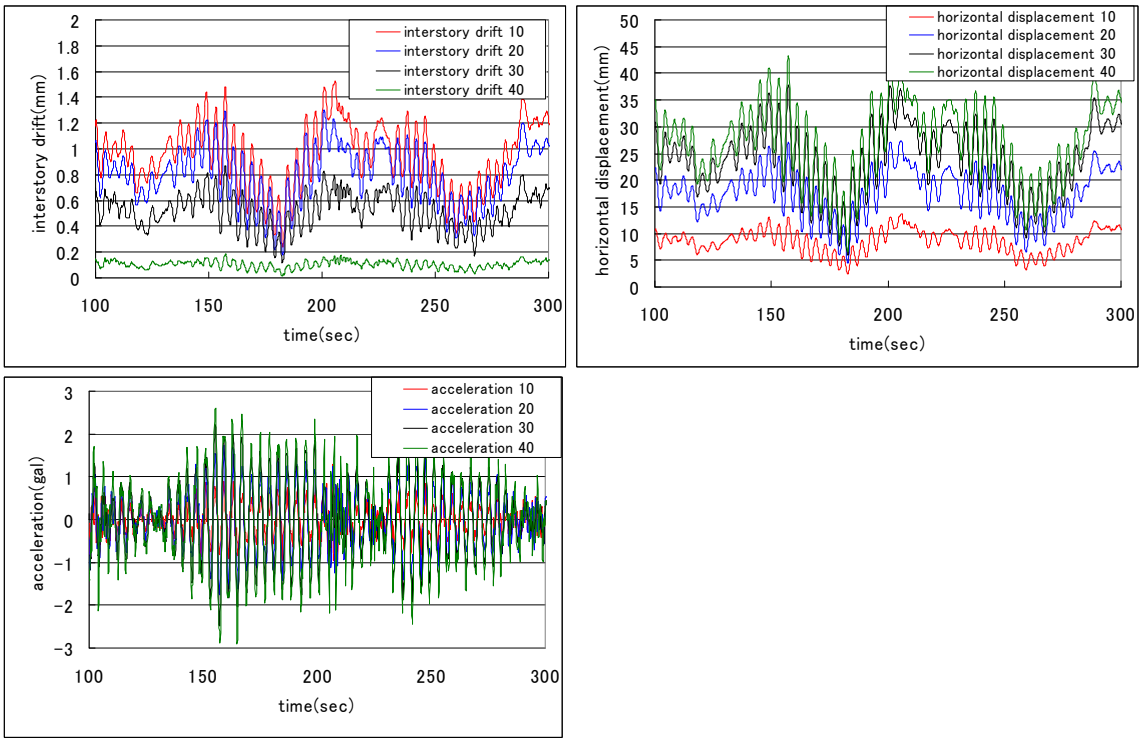

Fig.19 Time histories of interstory drifts, horizontal displacement and accelerations at several representative floors (10, 20, 30, 40th stories) of the building without damper subjected to along-wind disturbances of Level 0

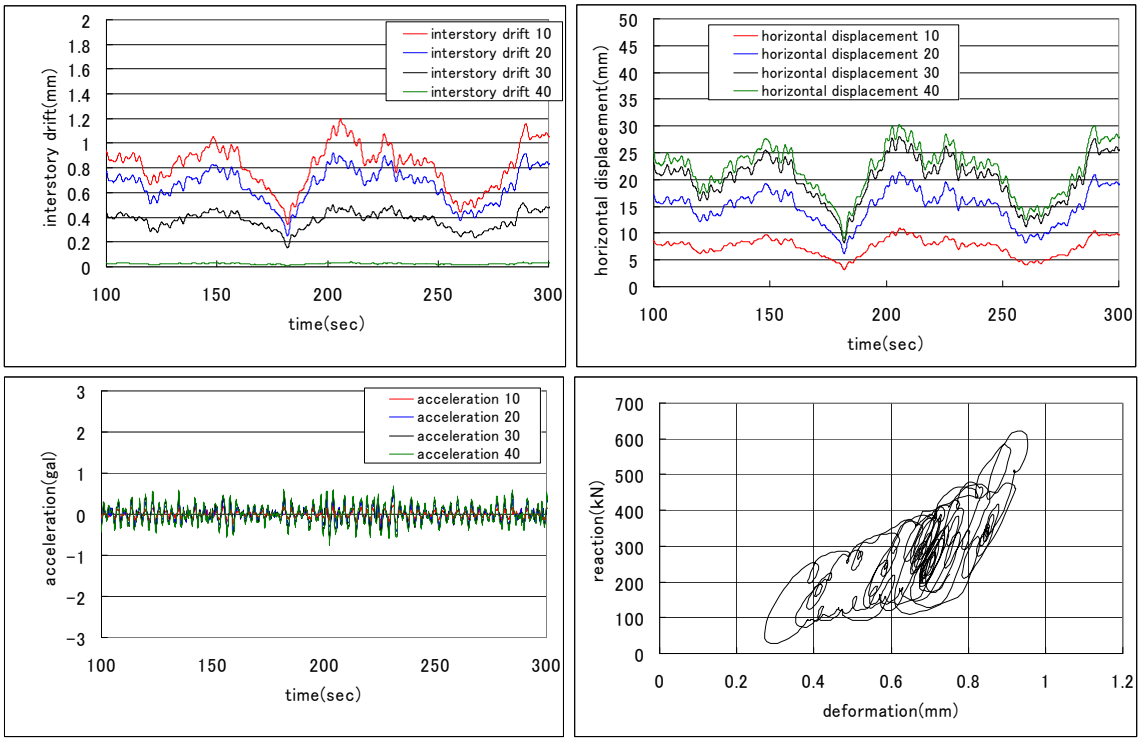

Fig.20 Time histories of interstory drifts, horizontal displacement and accelerations at several representative floors (10, 20, 30, 40th stories) of the building with 4 rubber dampers subjected to along-wind disturbances of Level 0. Total reaction force of the dampers in the 10th story is also plotted with respect to shear deformation of the dampers.

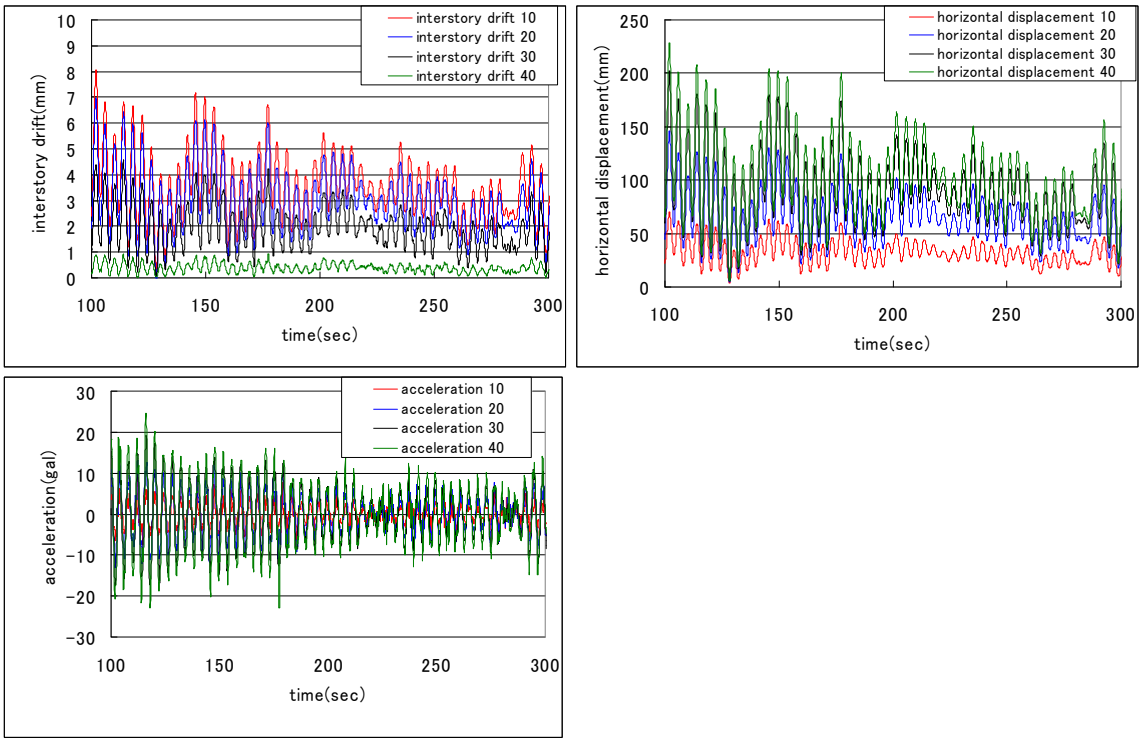

Fig.21 Time histories of interstory drifts, horizontal displacement and accelerations at several representative floors (10, 20, 30, 40th stories) of the building without damper subjected to along-wind disturbances of Level 1

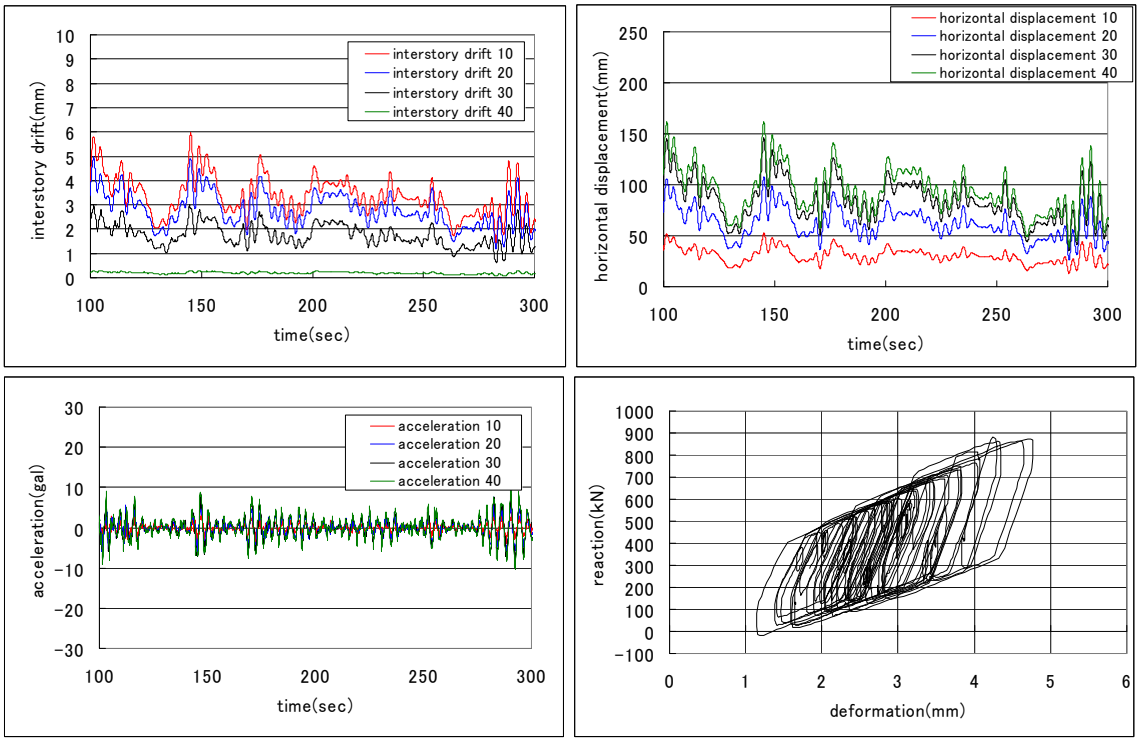

Fig.22 Time histories of interstory drifts, horizontal displacement and accelerations at several representative floors (10, 20, 30, 40th stories) of the building with 4 rubber dampers subjected to along-wind disturbances of Level 1. Total reaction force of the dampers in the 10th story is also plotted with respect to shear deformation of the dampers.

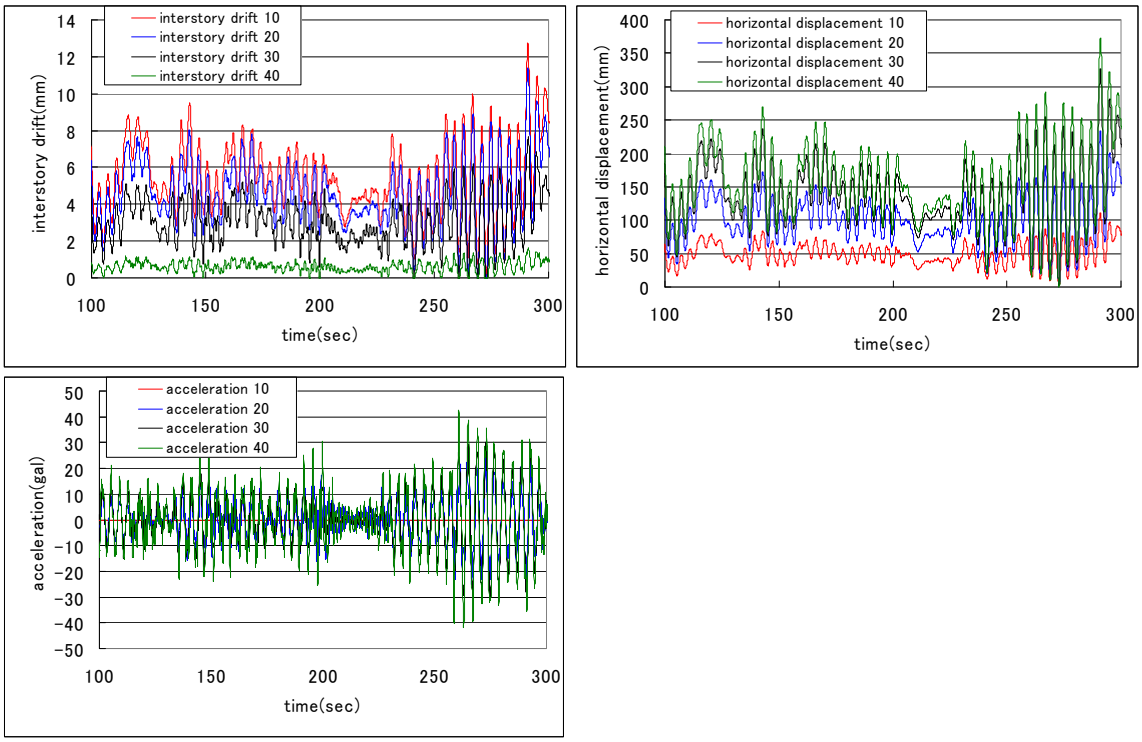

Fig.23 Time histories of interstory drifts, horizontal displacement and accelerations at several representative floors (10, 20, 30, 40th stories) of the building without damper subjected to along-wind disturbances of Level 2

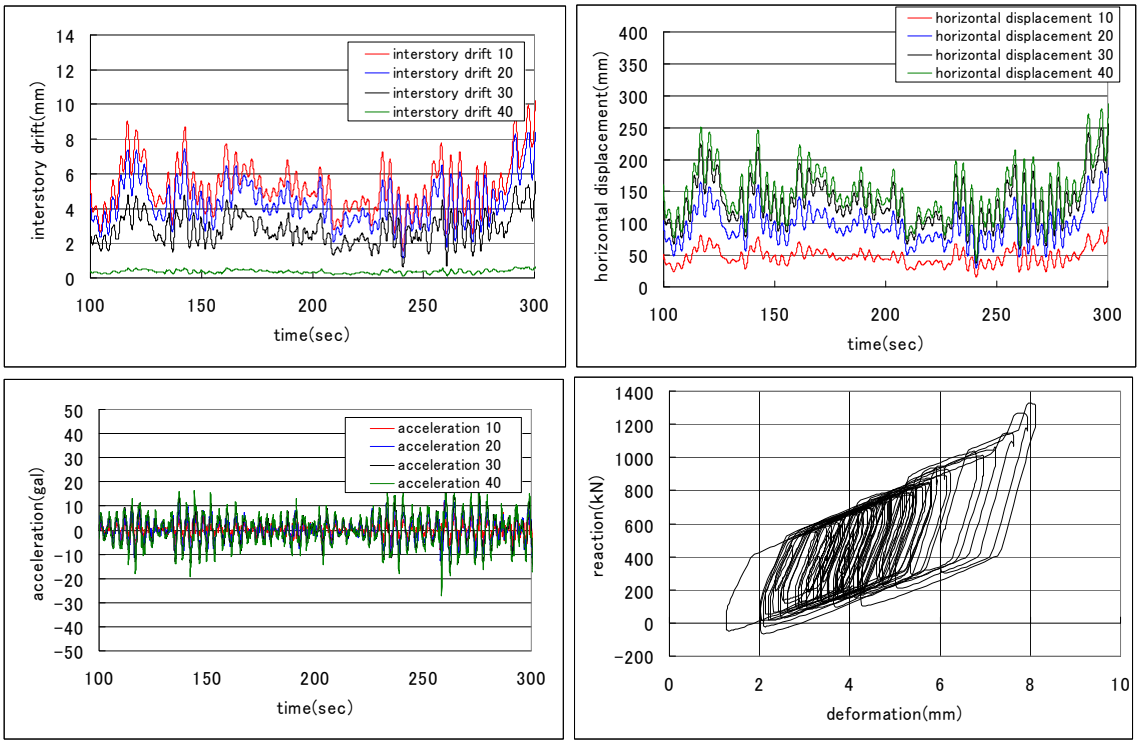

Fig.24 Time histories of interstory drifts, horizontal displacement and accelerations at several representative floors (10, 20, 30, 40th stories) of the building with 4 rubber dampers subjected to along-wind disturbances of Level 2. Total reaction force of the dampers in the 10th story is also plotted with respect to shear deformation of the dampers.

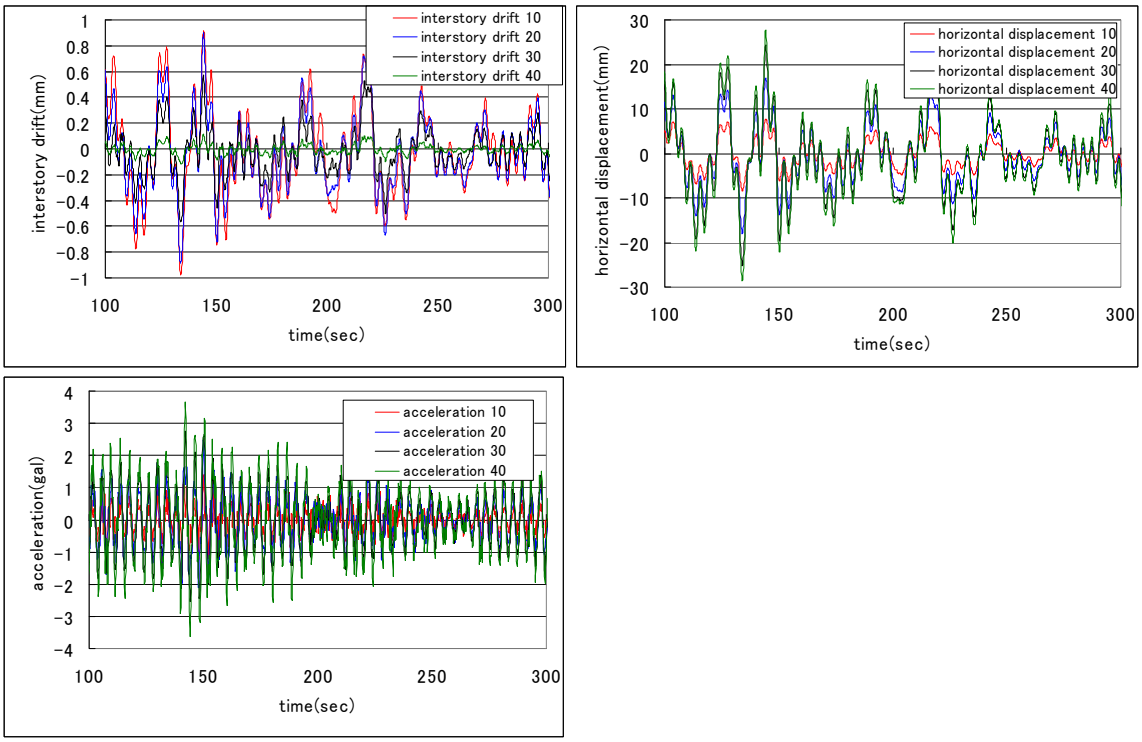

Fig.25 Time histories of interstory drifts, horizontal displacement and accelerations at several representative floors (10, 20, 30, 40th stories) of the building without damper subjected to cross-wind disturbances of Level 0

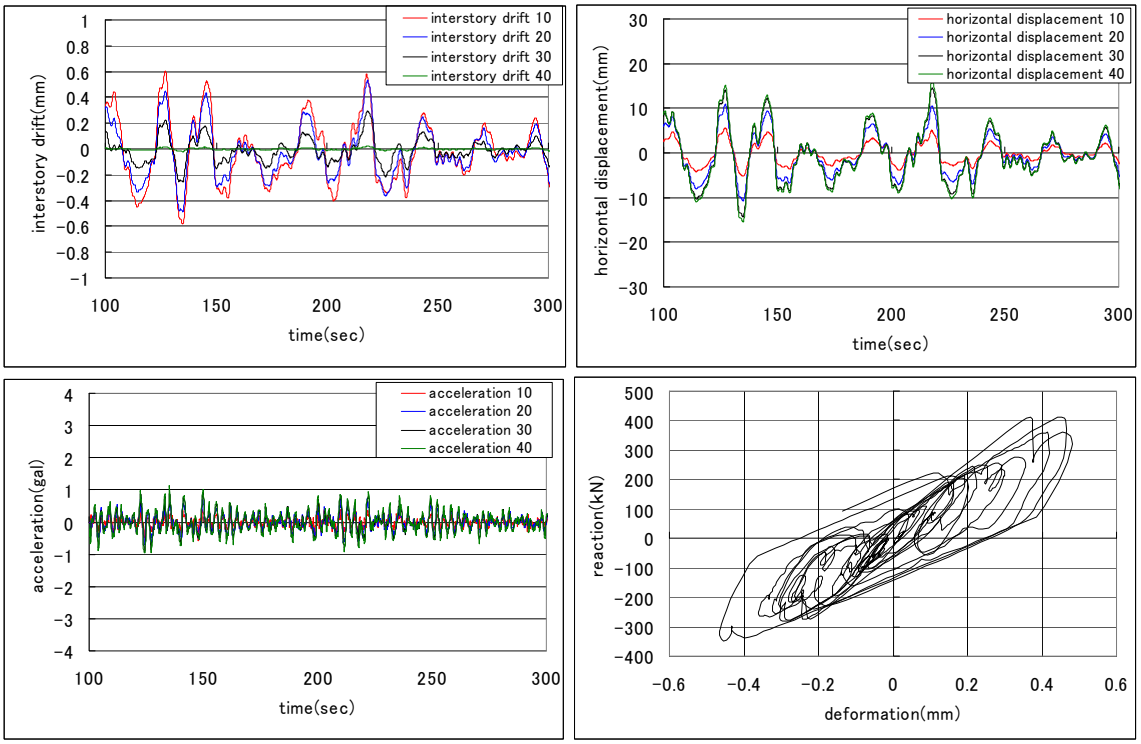

Fig.26 Time histories of interstory drifts, horizontal displacement and accelerations at several representative floors (10, 20, 30, 40th stories) of the building with 4 rubber dampers subjected to cross-wind disturbances of Level 0. Total reaction force of the dampers in the 10th story is also plotted with respect to shear deformation of the dampers.

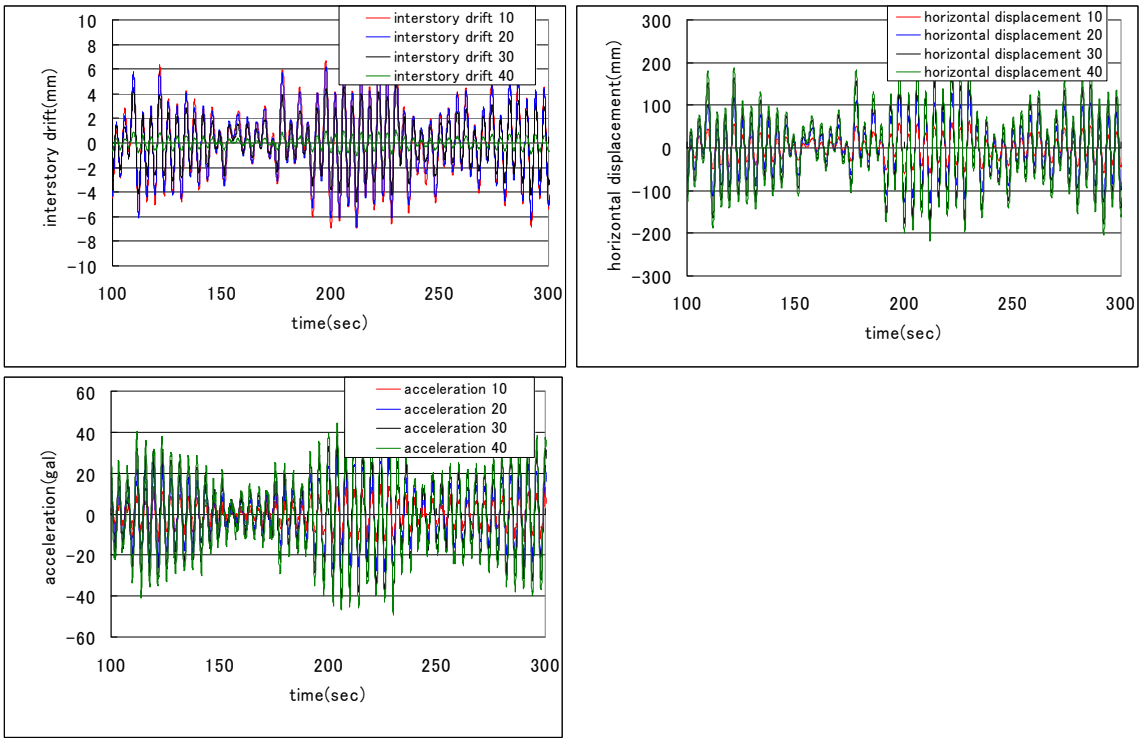

Fig.27 Time histories of interstory drifts, horizontal displacement and accelerations at several representative floors (10, 20, 30, 40th stories) of the building without damper subjected to cross-wind disturbances of Level 1

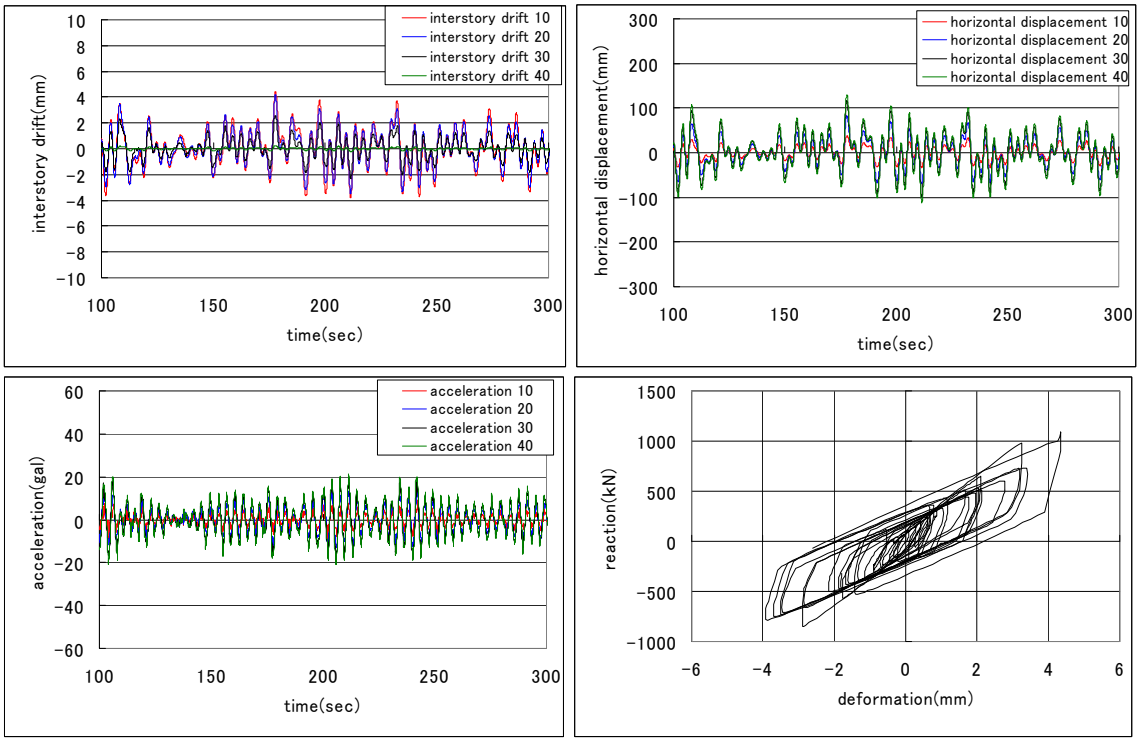

Fig.28 Time histories of interstory drifts, horizontal displacement and accelerations at several representative floors (10, 20, 30, 40th stories) of the building with 4 rubber dampers subjected to cross-wind disturbances of Level 1. Total reaction force of the dampers in the 10th story is also plotted with respect to shear deformation of the dampers.

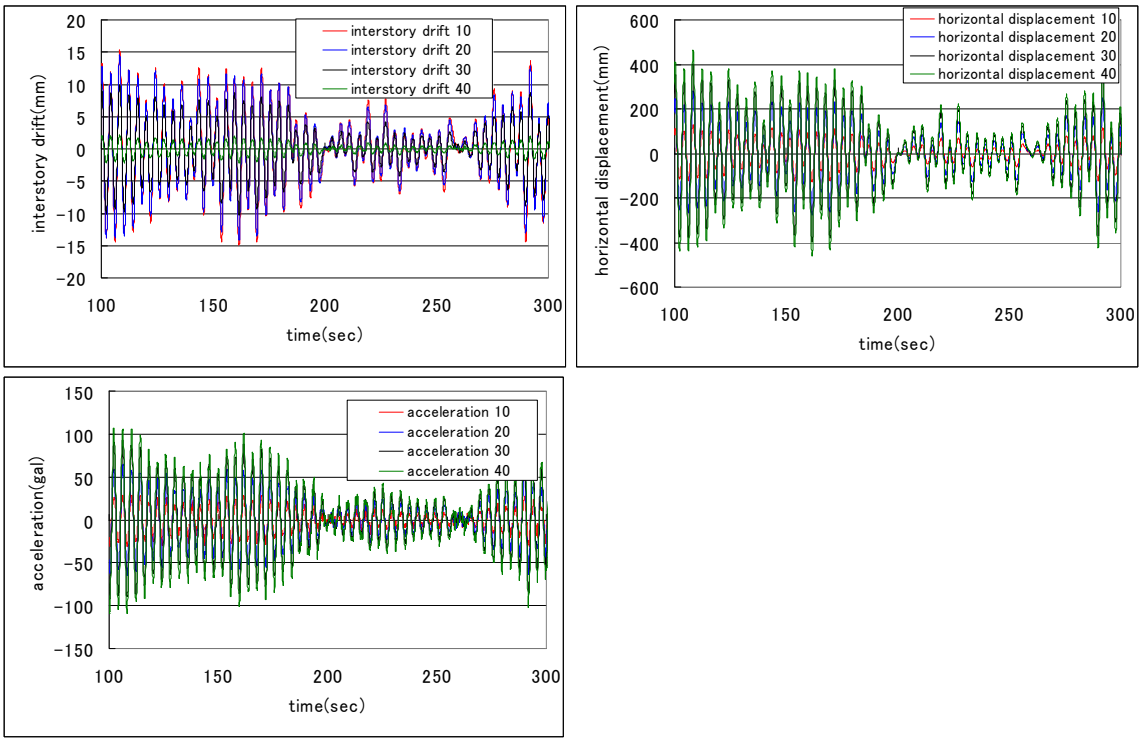

Fig.29 Time histories of interstory drifts, horizontal displacement and accelerations at several representative floors (10, 20, 30, 40th stories) of the building without damper subjected to cross-wind disturbances of Level 2

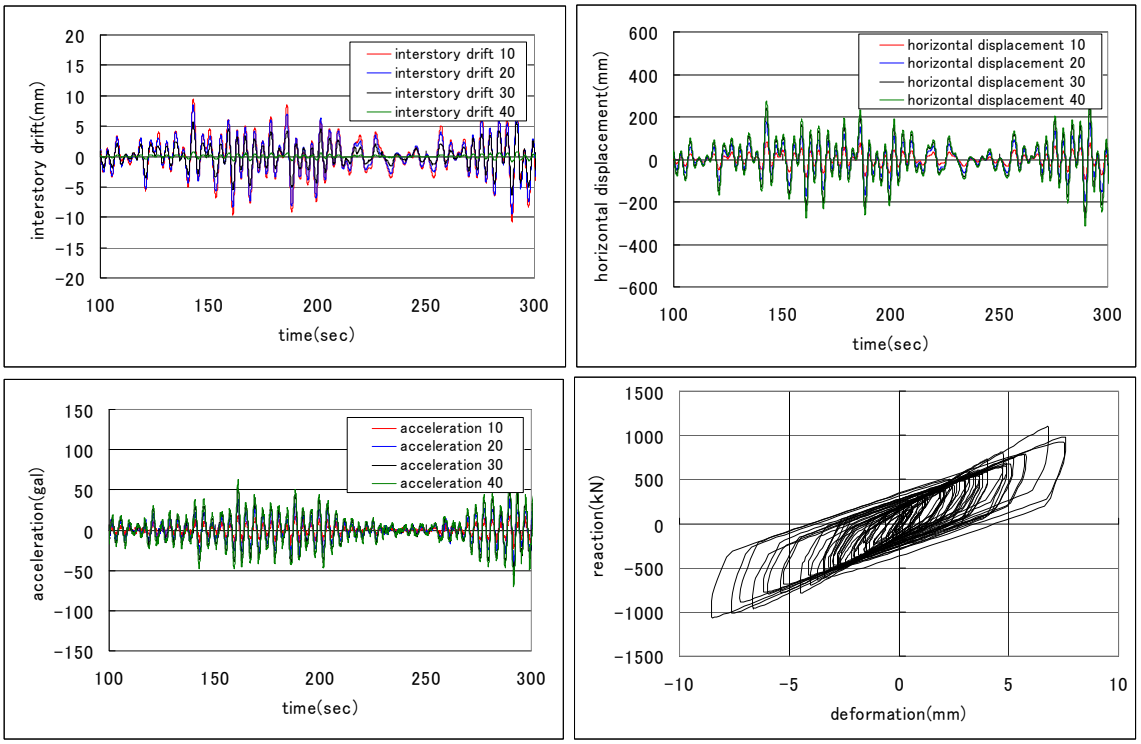

Fig.30 Time histories of interstory drifts, horizontal displacement and accelerations at several representative floors (10, 20, 30, 40th stories) of the building with 4 rubber dampers subjected to cross-wind disturbances of Level 2. Total reaction force of the dampers in the 10th story is also plotted with respect to shear deformation of the dampers.

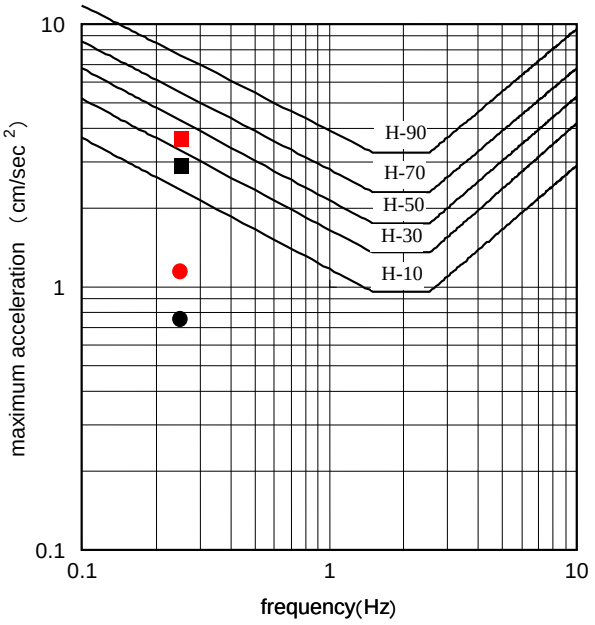

Fig.31 Assessment check of habitability environment of the buildings with (circle) and without (square) the proposed high-hardness rubber dampers for wind loading of Level 0 (black: along-wind, red: cross-wind)

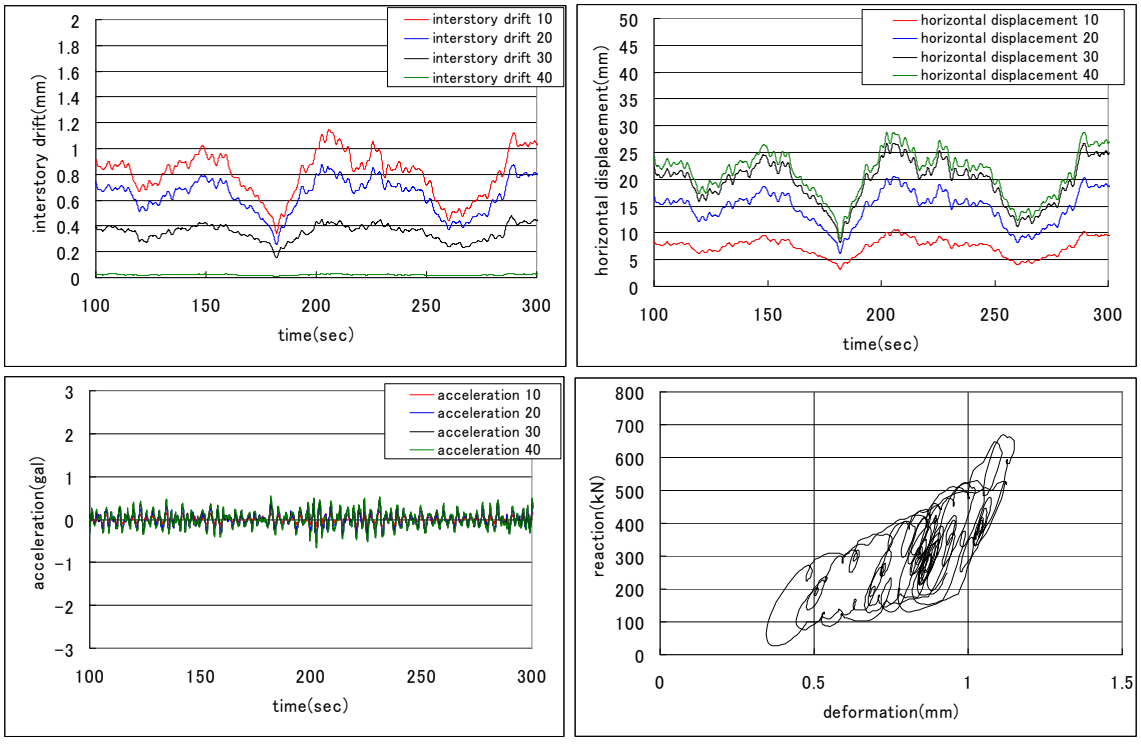

Fig.32 Time histories of interstory drifts, horizontal displacement and accelerations at several representative floors (10, 20, 30, 40th stories) of the building with 4 rubber dampers subjected to along-wind disturbances of Level 0. Total reaction force of the dampers in the 10th story is also plotted with respect to shear deformation of the dampers. The effect is not included of overall flexural deformation of the frame on the performance of the rubber damper.